Supporting Information

Binder free construction of hollow hierarchical Mn-Co-P nanoarrays on nickel foam as an efficient bifunctional electrocatalyst for overall water splitting

Fan Wang[a], Xingzhong Guo[a,c], Fan He[b], Yang Hou[b], Fu Liu[a], Chang Zou[a], Hui Yang[a]*

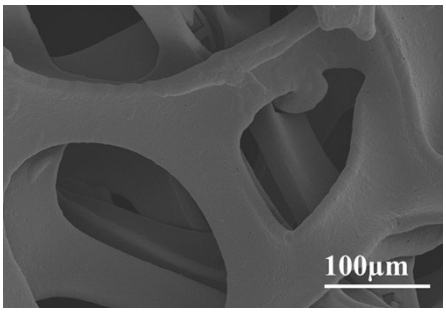

Figure S1. FESEM images of nickel foam.

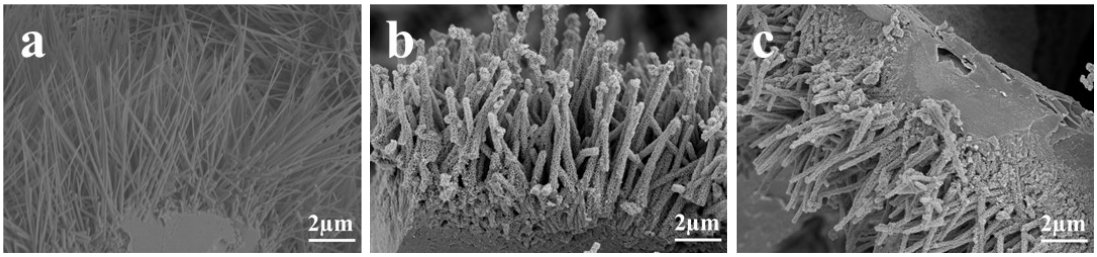

Figure S2. FESEM images of (a) Co precursor, (b) Mn-Co precursor and (c) Mn-Co-P nanoarrays.

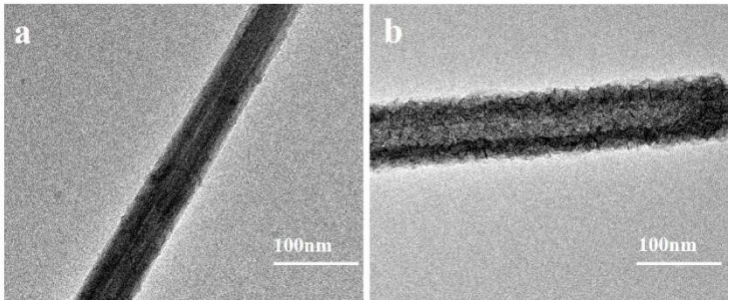

Figure S3. TEM images of (a) Co precursor and (b) Mn-Co precursor nanoarrays.

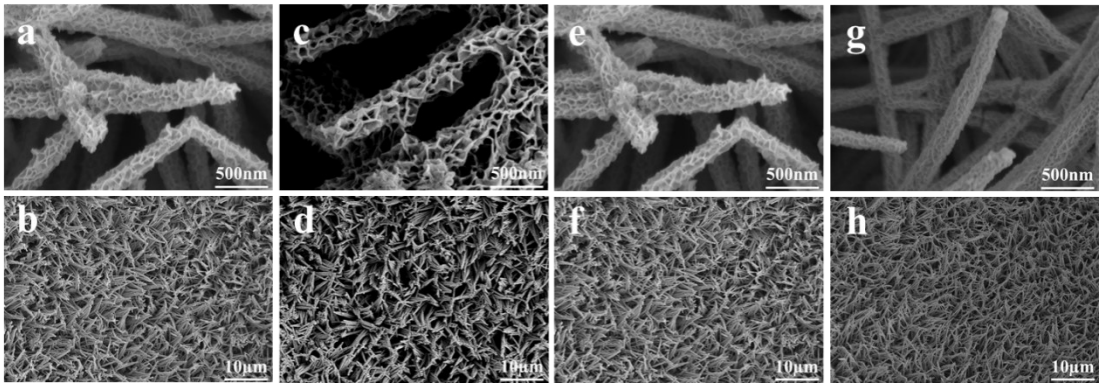

Figure S4. FESEM images of Mn-Co-P nanoarrays with different Mn contents: (a, b) 0.005 M, (c, d) 0.01 M, (e, f) 0.05 M and (g, h) 0.1 M.

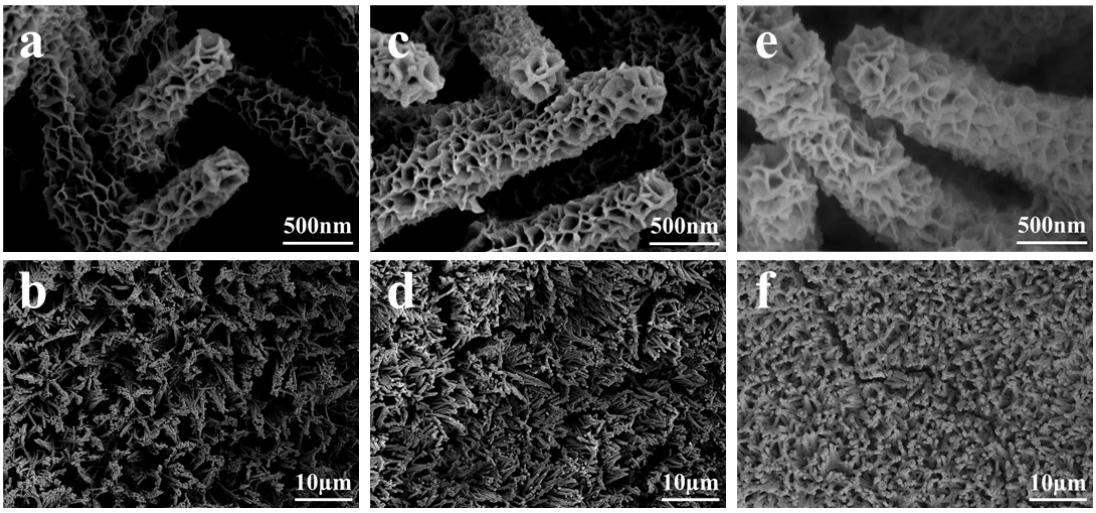

Figure S5. FESEM images of Mn-Co-P nanoarrays with different reaction time: (a, b) 3 h, (c, d) 5 h and (e, f) 10 h.

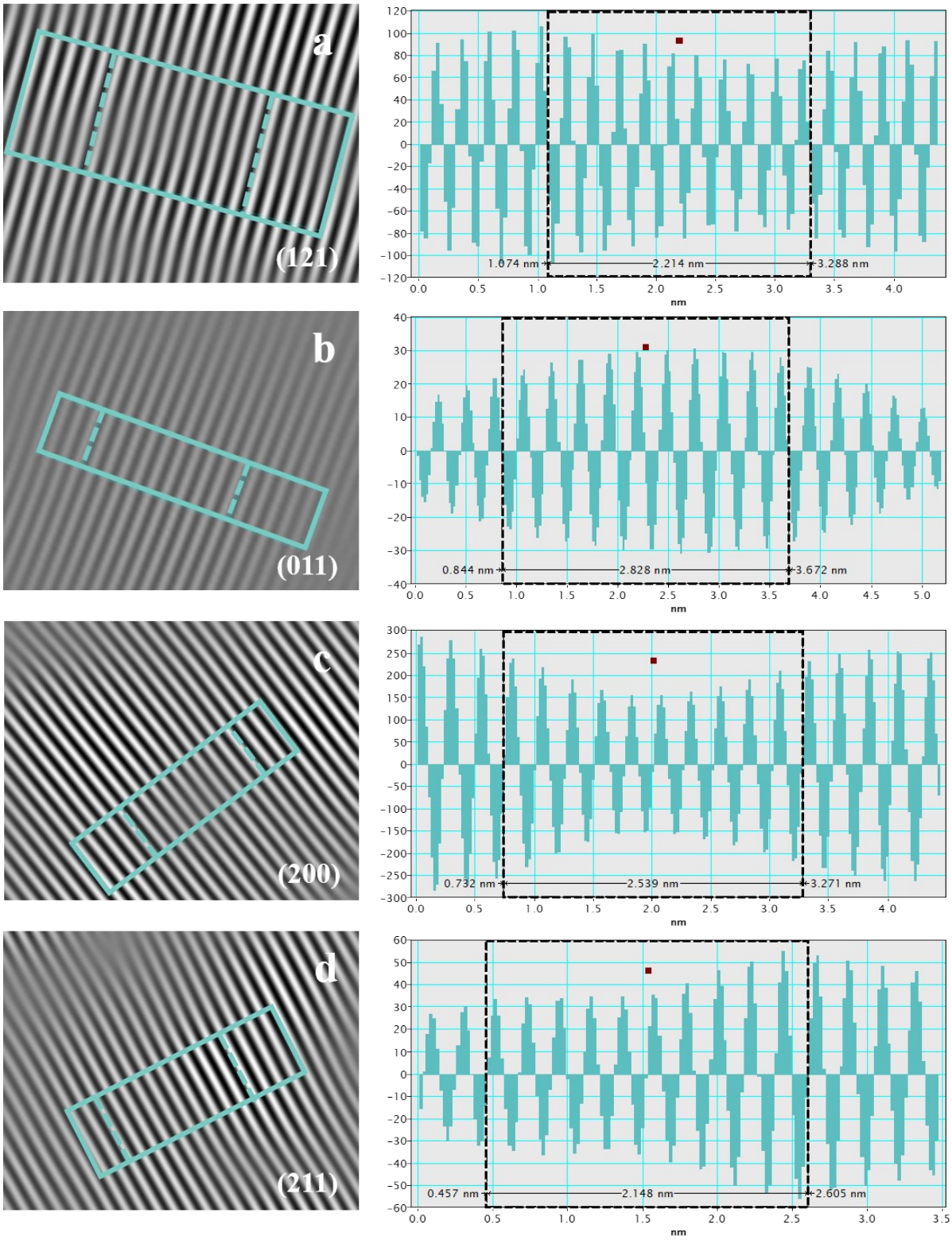

Figure S6. HRTEM images of Mn-Co-P nanoarrays.

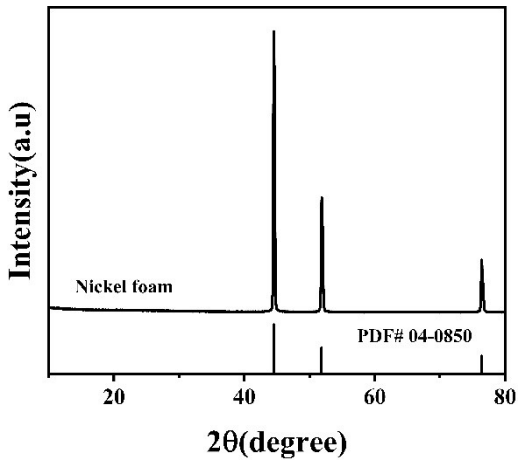

Figure S7. XRD pattern of nickel foam.

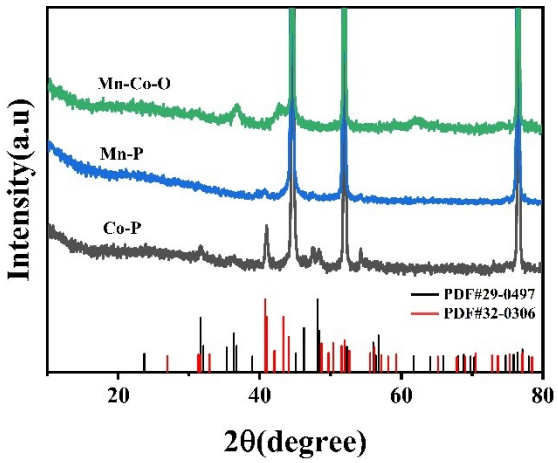

Figure S8. XRD patterns of Co-P, Mn-P and Mn-Co-O nanoarrays.

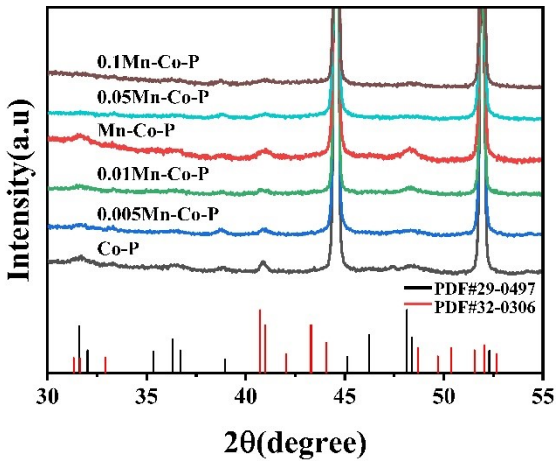

Figure S9. XRD patterns of Co-P and Mn-Co-P nanoarrays with different Mn contents.

Table S1. Metal-atomic content detected by ICP-MS analysis.

Catalysts	Mn (at. %)	Co (at. %)	P (at. %)
Mn-Co precursor	2.73	9.58	
Mn-Co-P	2.65	8.71	8.48

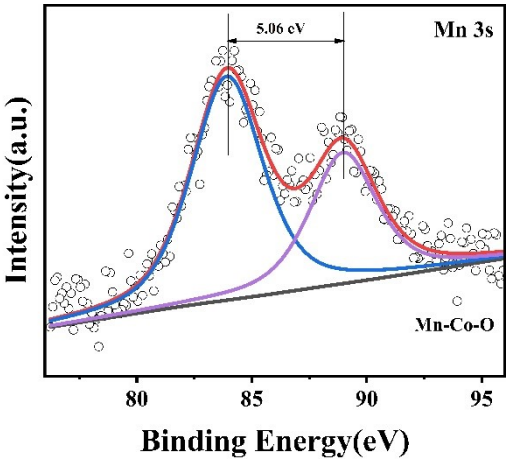

Figure S10. High-resolution XPS spectra of Mn-Co-O for Mn 3s.

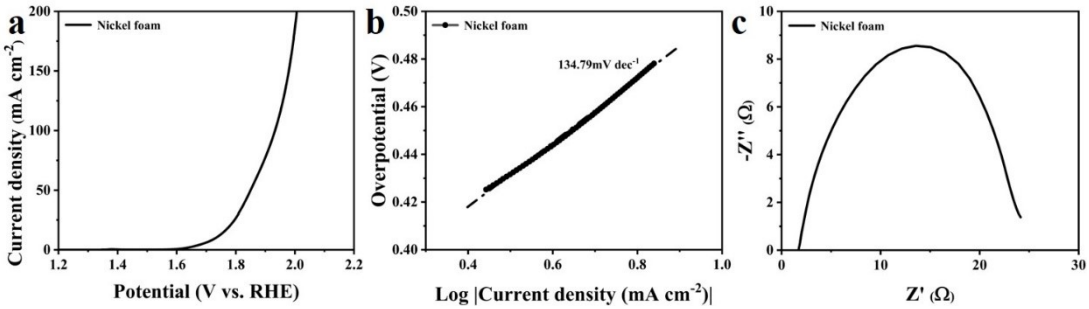

Figure S11. OER performance curves of nickel foam: (a) LSV, (b) the corresponding Tafel slope and (c) Nyquist plot.

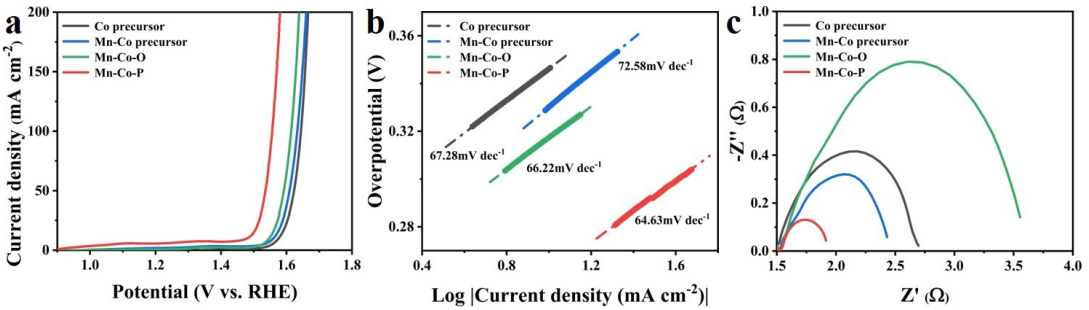

Figure S12. (a) LSV curves, (b) the corresponding Tafel plots and (c) Nyquist plots of Co precursor, Mn-Co precursor, Mn-Co-O and Mn-Co-P nanoarrays towards OER.

Table S2. Comparison of the OER performances of hollow hierarchical Mn-Co-P nanoarrays with the previously reported electrocatalysts at alkaline media.

Electrocatalysts	Overpotential (mV) at 10 mA cm^{-2}	Overpotential (mV) at 100 mA cm^{-2}	Tafel slop (mV dec^{-1})	Reference
Hollow hierarchical Mn-Co-P nanoarrays	250	326	64.63	This work
CoMn-LDHs	395		45	[1]
MnO/Co/PGC	301		77	[2]
CoMn-LDH@g-C_3N_4	303		48	[3]
N-CoO@CoP		332	81.5	[4]
Cu@CoP	270		77.2	[5]
CoFeBiP	273		77.3	[6]
Mn-Co-P/NF	310		194	[7]
Ni-Fe-$K_{0.23}MnO_2$ CNFs-300	270	320	42.3	[8]
Mn_3O_4/CoP	306		51.8	[9]
MnCo@NiS	286		31.5	[10]
Mn-Co phosphide yolk-shell spheres	330		59	[11]
MnCoP/CC	261	460	44.9	[12]
$Mn_{0.6}Co_{0.4}P$-rGO	250		65	[13]
Mn-CoP nanosheets	290		76	[14]
Mn (5%)-CoP/CC	317		67.1	[15]
CoMnP nanoparticles	330		61	[16]

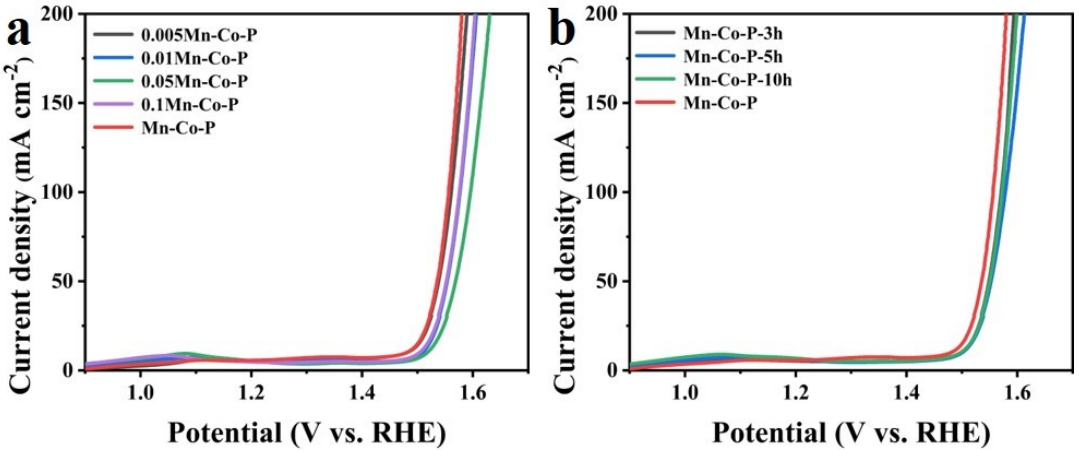

Figure S13. LSV curves of Mn-Co-P nanoarrays for (a) different Mn contents and (b) different reaction time towards OER.

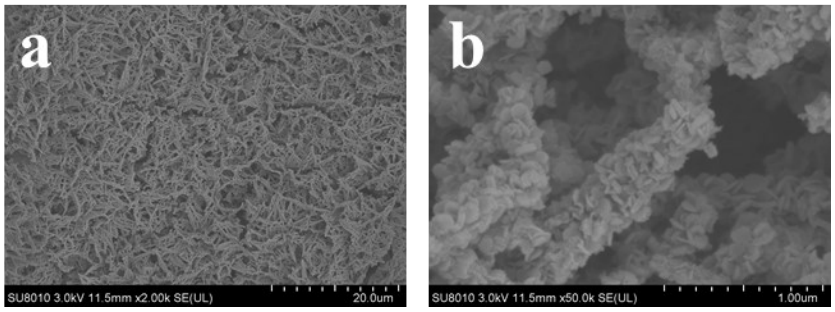

Figure S14. (a, b) FESEM images of hollow hierarchical Mn-Co-P nanoarrays after 72 h chronopotentiometry test towards OER.

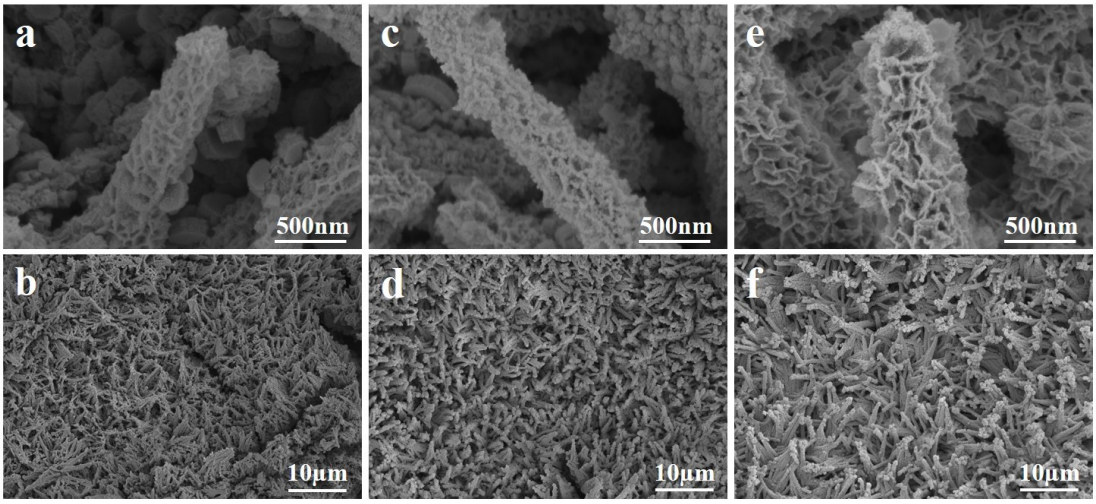

Figure S15. FESEM images of Mn-Co-P nanoarrays with different reaction time: (a, b) 3 h, (c, d) 5 h and (e, f) 10 h after LSV test towards OER.

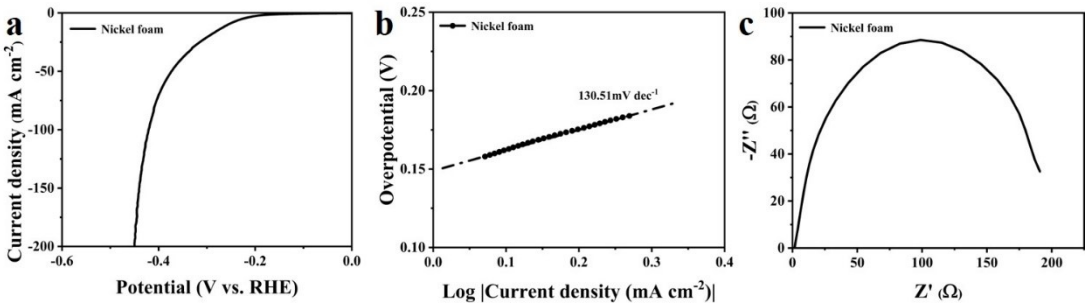

Figure S16. HER performance curves of nickel foam: (a) LSV, (b) the corresponding Tafel slope and (c) Nyquist plot.

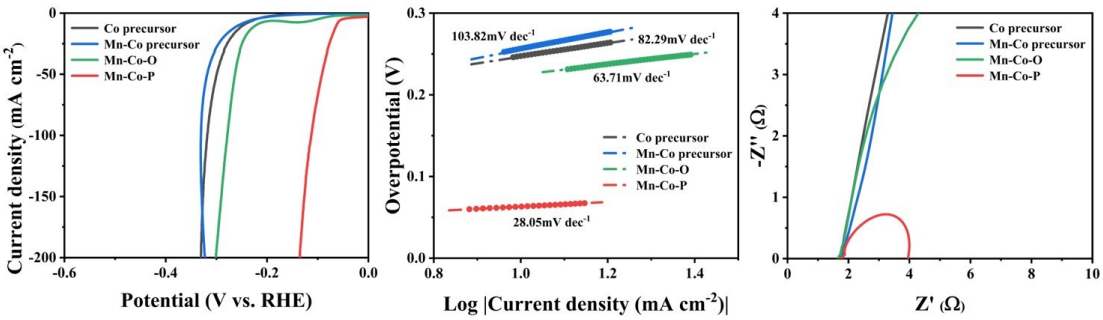

Figure S17. (a) LSV curves, (b) the corresponding Tafel plots and (c) Nyquist plots of Co precursor, Mn-Co precursor, Mn-Co-O and Mn-Co-P nanoarrays towards HER.

Table S3. Comparison of the HER performances of hollow hierarchical Mn-Co-P nanoarrays with the previously reported electrocatalysts at alkaline media.

Electrocatalysts	Overpotential (mV) at 10 mA cm^{-2}	Overpotential (mV) at 100 mA cm^{-2}	Tafel slop (mV dec^{-1})	Reference
Hollow hierarchical Mn-Co-P nanoarrays	63	112	28.05	This work
Mn-Co-P/Ti	76		52	[17]
Co_1Mn_1Se NBs	87.3		71.2	[18]
CoMn-LDH@g-C_3N_4	406		59	[3]
N-CoO@CoP		201	37	[4]
Cu@CoP	88		51.6	[5]
Mn-Co-P/NF	63		114	[7]
Mn_3O_4/CoP	43		28.9	[9]
CoNiMn/NC	191		64.38	[19]
Mn-N-Co_9S_8	102	238	107.2	[20]
Ni-Fe-$K_{0.23}MnO_2$ CNFs-300	116	242	103.9	[8]
CoMn-P@NG	164		111	[21]
MnCoP/CC	65		46.16	[12]
Mn-O@CoP	106		56	[22]
$Mn_{0.6}Co_{0.4}P$-rGO	54		63	[13]
Mn-Co-P	66		82	[23]
Mn-CoP nanosheets	195		69	[14]
Mn-CoP	95			[24]
Mn doped CoP	100		53	[25]

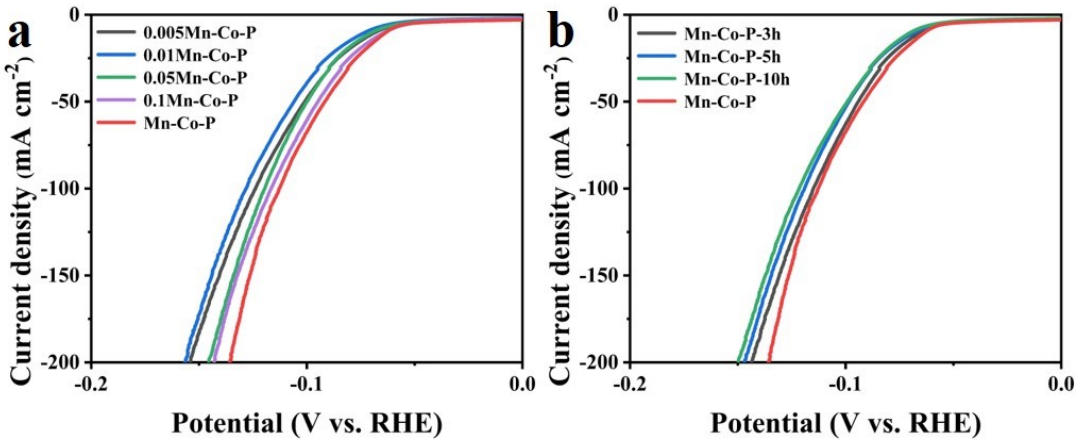

Figure S18. LSV curves of Mn-Co-P nanoarrays for (a) different content of Mn and (b) different reaction time of Mn towards HER.

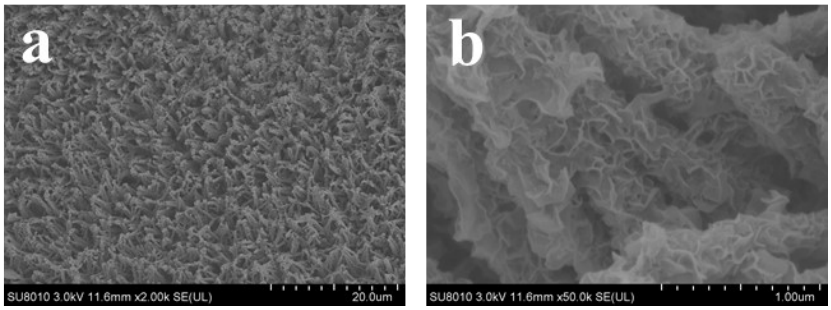

Figure S19. (a, b) FESEM images of hollow hierarchical Mn-Co-P nanoarrays after 72 h chronopotentiometry test towards HER.

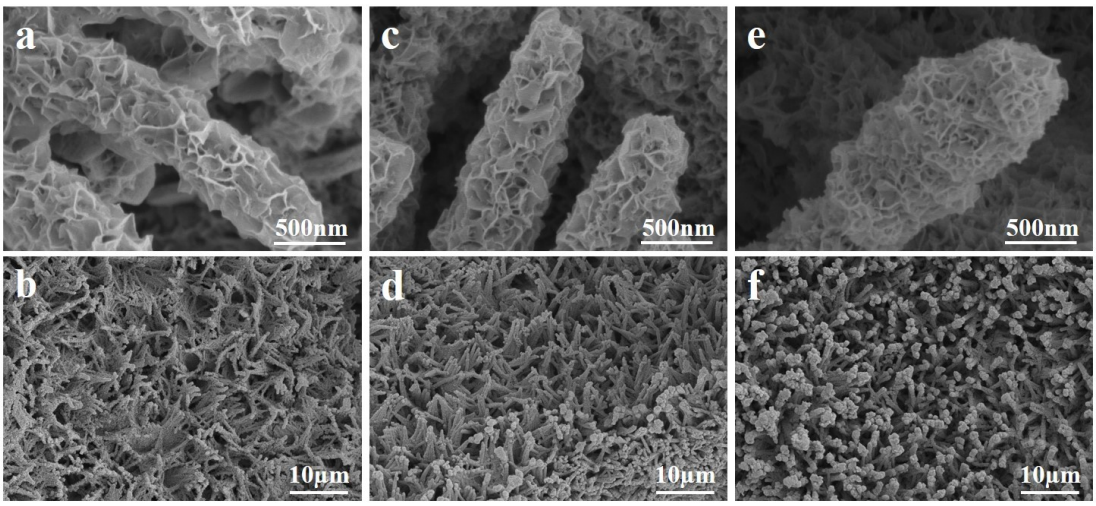

Figure S20. FESEM images of Mn-Co-P nanoarrays with different reaction time: (a, b) 3 h, (c, d) 5 h and (e, f) 10 h after LSV test towards HER.

Table S4. Comparison of overall water splitting performances of hollow hierarchical Mn-Co-P nanoarrays with previously reported electrocatalysts at alkaline media.

Electrocatalysts	Voltage (V) at 10 mA cm^{-2}	Voltage (V) at 100 mA cm^{-2}	Reference
Hollow hierarchical Mn-Co-P nanoarrays	1.57	1.71	This work
Co_1Mn_1Se NBs	1.60		18
Co_2Mn_1 DH	1.65		26
CoMn-LDH@g-C_3N_4	1.62		3
N-CoO@CoP		1.79	4
Cu@CoP	1.65		5
Mn_3O_4/CoP	1.599		9
MnFeO-NF	1.59		27
Ni-Fe-$K_{0.23}MnO_2$ CNFs-300	1.62	1.81	8
MnCoP/CC	1.68		12
$Mn_{0.6}Co_{0.4}P$-rGO	1.55	1.77	13
Mn-Co-P	1.74		23

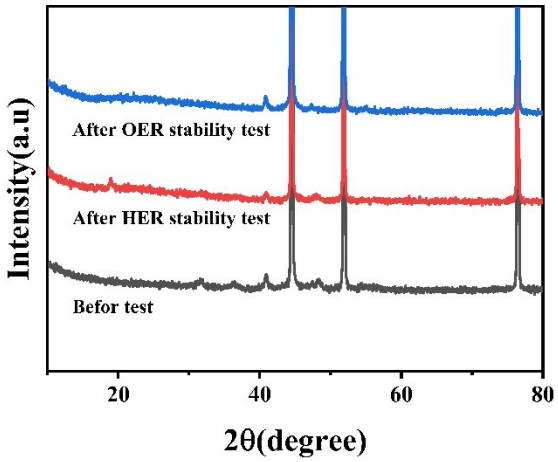

Figure S21. XRD patterns of hollow hierarchical Mn-Co-P nanoarrays before test, after HER stability test and after OER stability test.

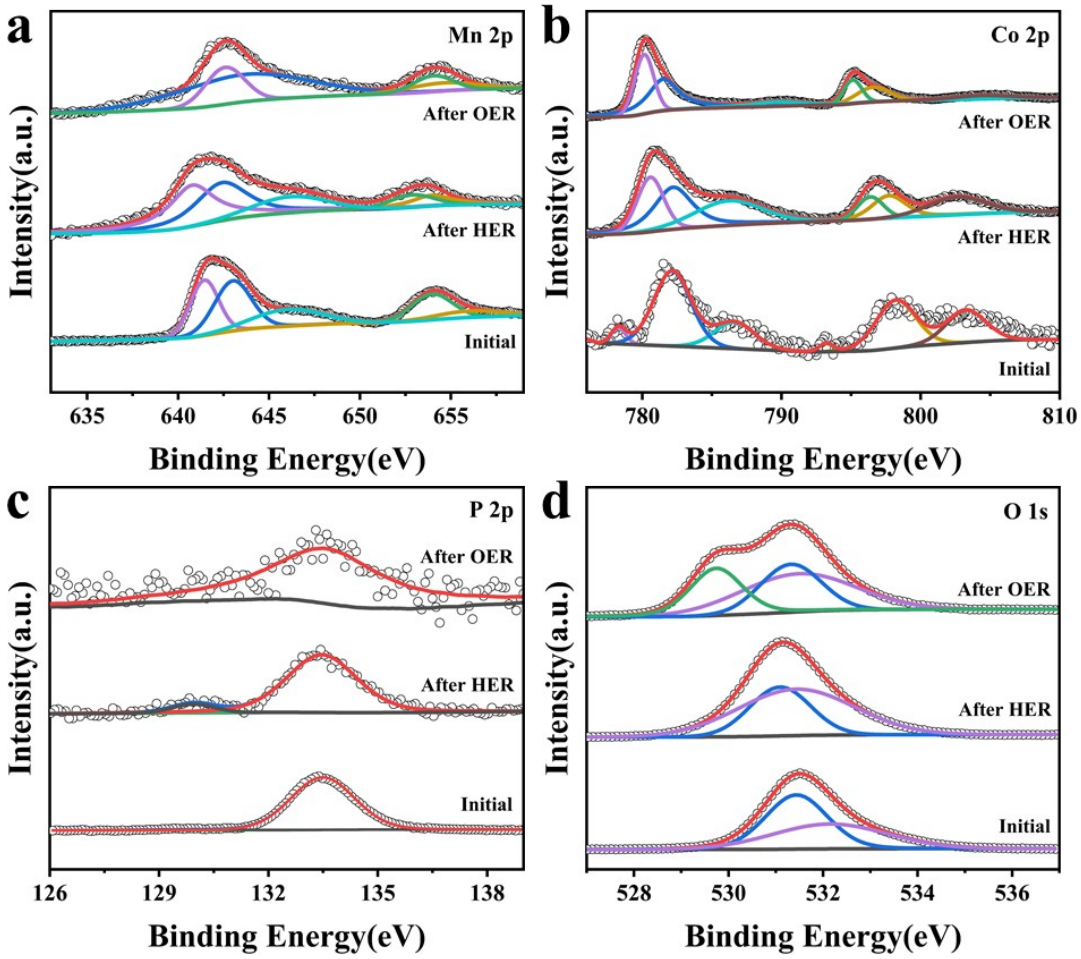

Figure S22. XPS spectra of (a) Mn 2p, (b) Co 2p, (c) P 2p and (d) O 1s of hollow hierarchical Mn-Co-P nanoarrays before test, after HER stability test and after OER stability test.

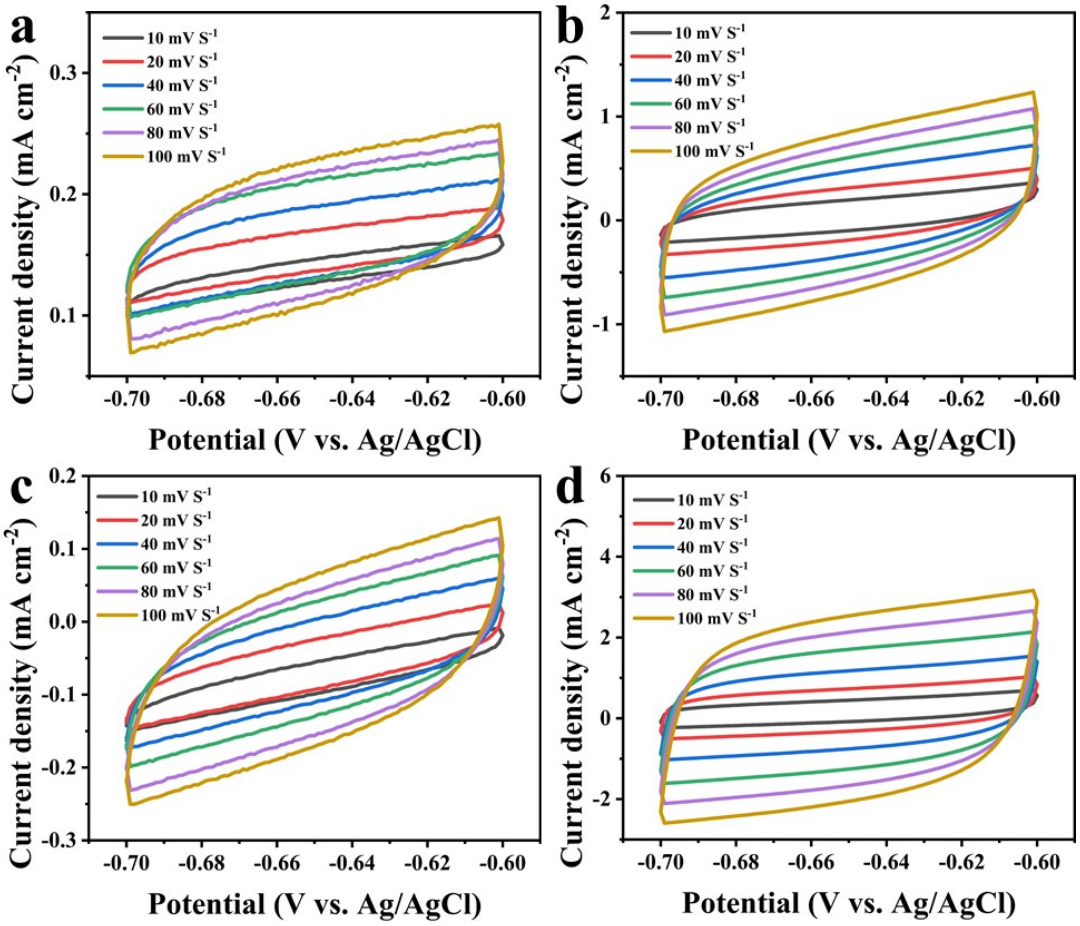

Figure S23. CV curves of (a) nickel foam, (b) Co-P, (c) Mn-P, and (d) Mn-Co-P nanoarrays at different scan rates (10, 20, 40, 60, 80 and 100 mV s^{-1}) in the non-faradaic potential region of -0.7 to -0.6 V *vs*. Ag/AgCl.

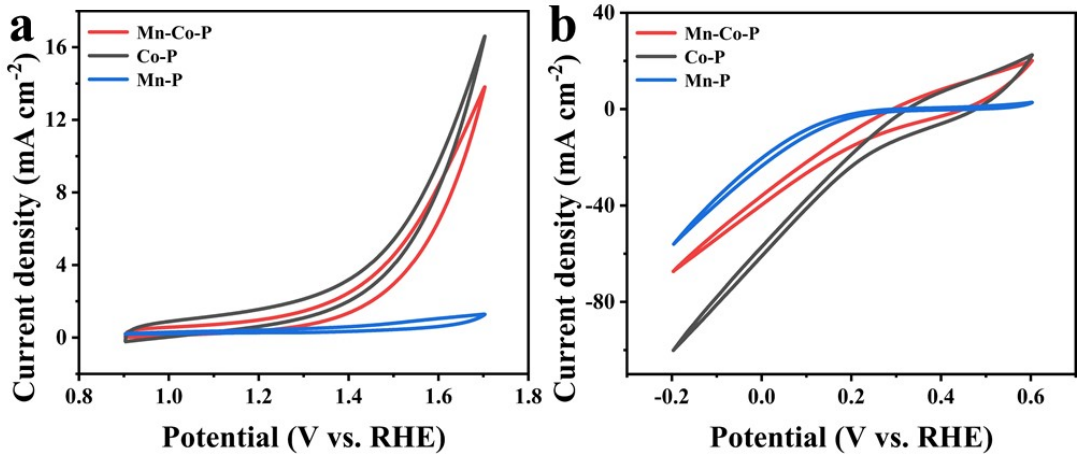

Figure S24. CV curves of Co-P, Mn-P and Mn-Co-P nanoarrays at a scan rate of 50 mV s^{-1} in 1.0 M PBS (pH=7) for (a) OER and (b) HER.

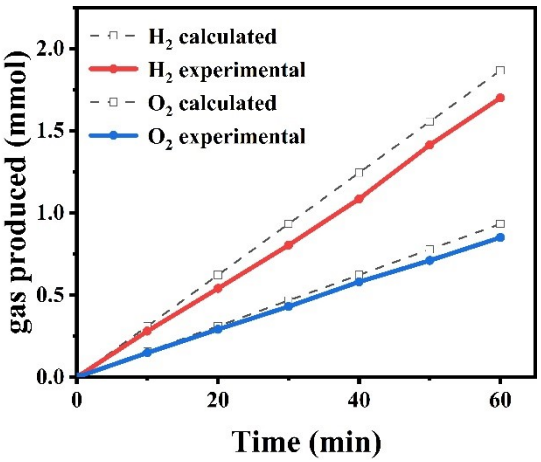

Figure S25. The quantity of gas theoretically calculated and experimentally measured versus time employing hollow hierarchical Mn-Co-P nanoarrays as both anode and cathode at current density of 100 mA cm^{-2}.

References

1. Z. Yi, C. Ye, M. Zhang, Y. Lu, Y. Liu, L. Zhang and K. Yan, *Appl. Surf. Sci.*, 2019, **480**, 256-261.
2. X. F. Lu, Y. Chen, S. Wang, S. Gao and X. W. D. Lou, *Adv. Mater.*, 2019, **31**, e1902339.
3. M. Arif, G. Yasin, M. Shakeel, X. Fang, R. Gao, S. Ji and D. Yan, *Chem. Asian. J.*, 2018, **13**, 1045-1052.
4. M. Lu, L. Li, D. Chen, J. Li, N. I. Klyui and W. Han, *Electrochim. Acta*, 2020, **330**, 135210.
5. P. Wang, Y. Lin, L. Wan and B. Wang, *Energy & Fuels*, 2020, **34**, 10276-10281.
6. C. Wang, H. Shang, Y. Wang, J. Li, S. Guo, J. Guo and Y. Du, *Nanoscale*, 2021, **13**, 7279-7284.
7. Z. Feng, Y. Sui, Z. Sun, J. Qi, F. Wei, Y. Ren, Z. Zhan, M. Zhou, D. Meng, L. Zhang, L. Ma and Q. Wang, *Colloid Surface A*, 2021, **615**, 126265.
8. H. Liao, X. Guo, Y. Hou, H. Liang, Z. Zhou and H. Yang, *Small*, 2020, **16**, e1905223.
9. R. Dong, A. Zhu, W. Zeng, L. Qiao, L. Lu, Y. Liu, P. Tan and J. Pan, *Appl. Surf. Sci.*, 2021, **544**, 148860.
10. X. Wang, L. Li, L. Xu, Z. Wang, Z. Wu, Z. Liu and P. Yangs, *J. Power Sources*, 2021, **489**, 229525.
11. Y. V. Kaneti, Y. Guo, N. L. W. Septiani, M. Iqbal, X. Jiang, T. Takei, B. Yuliarto, Z. A. Alothman, D. Golberg and Y. Yamauchi, *Chem. Eng. J.*, 2021, **405**, 126580.
12. M. Wang, W. Fu, L. Du, Y. Wei, P. Rao, L. Wei, X. Zhao, Y. Wang and S. Sun, *Appl. Surf. Sci.*, 2020, **515**, 146059.
13. X. Xu, H. Liang, G. Tang, Y. Hong, Y. Xie, Z. Qi, B. Xu and Z. Wang, *Nanoscale Adv.*, 2019, **1**, 177-183.
14. Y. Li, B. Jia, B. Chen, Q. Liu, M. Cai, Z. Xue, Y. Fan, H. P. Wang, C. Y. Su and G. Li, *Dalton Trans.*, 2018, **47**, 14679-14685.
15. J. Lin, S. Xie, P. Liu, M. Zhang, S. Wang, P. Zhang and F. Cheng, *J. Mater. Res.*, 2017, **33**, 1258-1267.
16. D. Li, H. Baydoun, C. N. Verani and S. L. Brock, *J. Am. Chem. Soc.*, 2016, **138**, 4006-4009.

17. T. Liu, X. Ma, D. Liu, S. Hao, G. Du, Y. Ma, A. M. Asiri, X. Sun and L. Chen, *ACS Catal.*, 2016, **7**, 98-102.
18. H. Xu, J. Wei, K. Zhang, M. Zhang, C. Liu, J. Guo and Y. Du, *J. Mater. Chem. A*, 2018, **6**, 22697-22704.
19. B. Jiang and Z. Li, *J. Solid State Chem.*, 2021, **295**, 121912.
20. Y. Xing, D. Li, L. Li, H. Tong, D. Jiang and W. Shi, *Int. J. Hydrog. Energy*, 2021, **46**, 7989-8001.
21. J. Liu, W. Li, Z. Cui, J. Li, F. Yang, L. Huang, C. Ma and M. Zeng, *Chem. Commun. (Camb)*, 2021, **57**, 7200-2403.
22. D. Zhou, Z. Wang, X. Long, Y. An, H. Lin, Z. Xing, M. Ma and S. Yang, *J. Mater. Chem. A*, 2019, **7**, 22530-22538.
23. G. Tang, Y. Zeng, B. Wei, H. Liang, J. Wu, P. Yao and Z. Wang, *Energy Technol.*, 2019, **7**, 1900066.
24. X. Li, S. Li, A. Yoshida, S. Sirisomboonchai, K. Tang, Z. Zuo, X. Hao, A. Abudula and G. Guan, *Catal. Sci. Technol.*, 2018, **8**, 4407-4412.
25. Y. Ge, J. Chen, H. Chu, P. Dong, S. R. Craig, P. M. Ajayan, M. Ye and J. Shen, *ACS Sustain. Chem. Eng.*, 2018, **6**, 15162-15169.
26. K. Li, D. Guo, J. Kang, B. Wei, X. Zhang and Y. Chen, *ACS Sustain. Chem. Eng.*, 2018, **6**, 14641-14651.
27. J. Luo, W. H. Guo, Q. Zhang, X. H. Wang, L. Shen, H. C. Fu, L. L. Wu, X. H. Chen, H. Q. Luo and N. B. Li, *Nanoscale*, 2020, **12**, 19992-20001.